JOURNAL OF MATERIALS SCIENCE 19 (1984) 1947–1956

Failure processes in elastomers at or near a rigid spherical inclusion

A. N. GENT, BYOUNGKYEU PARK
Institute of Polymer Science, The University of Akron, Akron, Ohio 44325, USA

A systematic experimental study has been carried out of two distinct failure phenomena, cavitation and debonding, in an elastomer containing a rigid spherical inclusion. Several elastomers were employed containing glass beads of various diameters, ranging from 60 to 5000 μm, and with chemically different surfaces. The critical stress for cavitation was found to depend upon both Young's modulus, E, of the elastomer and the diameter of the bead. By extrapolation, it was found that the stress for cavitation near an infinitely-large bead is given by $5E/12$, as predicted by theory. In contrast, the critical stress for debonding decreased somewhat with increasing Young's modulus of the elastomer. This is attributed to a concomitant decrease in the strength of adhesion between the elastomer and the bead surface, due to rheological effects. The stresses for both cavitation and for debonding were found to vary approximately with the negative half-power of the bead diameter. This suggests that a similar Griffith mechanism governs both failure processes when the bead size is small. A study of cavitation and debonding in the presence of two glass beads was also carried out. As predicted from theoretical considerations, both stresses were found to decrease as the distance between the two beads was decreased, irrespective of the diameter of the bead and Young's modulus of the elastomer. At higher strains, however, a second cavitation process was found to take place at a point midway between the beads. Tensile fracture of the specimen resulted from the unrestrained lateral growth of the second cavity.

1. Introduction

Elastomers are commonly reinforced by the incorporation of relatively large amounts, 30 to 50 per cent by volume, of finely divided rigid fillers such as carbon black. The exact mechanism of reinforcement is still obscure, however. In an attempt to clarify it, a detailed study has now been carried out of the micromechanics of tensile failure in a sample containing a single rigid spherical inclusion. Some observations have also been made with two spherical inclusions placed close together in the direction of the applied tension, in order to study the effect of particle propinquity upon the mode of failure.

Two modes of failure have been noted previously in filled elastomers. When transparent elastomers containing fillers are stretched, vacuoles are commonly found to appear at a critical extension [1–3]. This phenomenon has been generally referred to as "dewetting" and attributed to detachment of weakly-bonded elastomer from the surface of filler particles. On the other hand, Oberth and Bruenner [4] showed that a small vacuole is formed near, but not at, the surface of a large rigid spherical inclusion when the elastomer was bonded to the inclusion sufficiently well to resist detachment. Elastomers undergo a characteristic failure process, termed cavitation, when subjected to a sufficiently large triaxial tension (negative hydrostatic pressure), given approximately by $5E/6$, where E is Young's modulus [5]. This process consists of the unbounded elastic expansion of a microvoid, assumed to be present initially in all elastomers, until material at its

0022–2461/84 $03.00 + .12 © *1984 Chapman and Hall Ltd.*

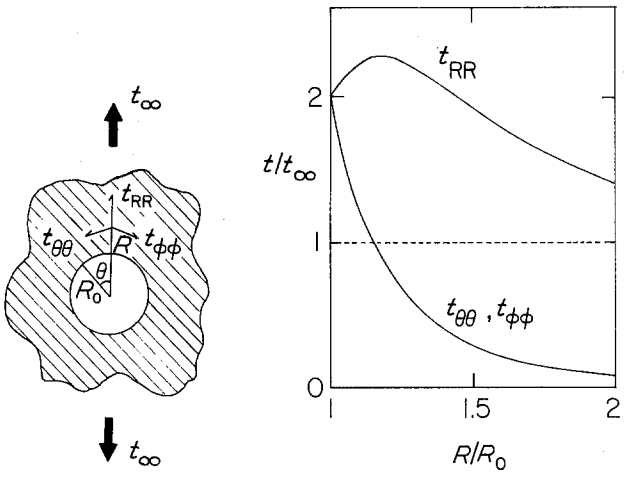

Figure 1 Stresses t_{RR}, $t_{\theta\theta}$, $t_{\phi\phi}$ near a rigid spherical inclusion as a function of distance from the surface of the inclusion in the direction of the applied tensile stress t_∞ [6].

surface reaches the breaking elongation. The cavity then grows in a catastrophic way until it is large enough to relieve the triaxial tension by its presence.

A triaxial tension is developed near the poles of a spherical inclusion, of magnitude $2t_\infty$ where t_∞ is the tensile stress applied at infinity [6], Fig. 1. We therefore expect vacuoles to appear near the poles of the inclusion when the applied stress reaches a value of $5E/12$. Oberth and Bruenner observed a direct proportionality between the stress for vacuole formation and Young's modulus of approximately this form, i.e. $E/2$, by experiments with polyurethane elastomers having a wide range of values of Young's modulus E, containing a single spherical inclusion with a diameter of about 6 mm. They also found that dewetting took place subsequently, if at all, by growth of cavities towards the surface of the inclusion.

Thus, for well-bonded systems the initial failure appears to take place near the inclusion by internal rupture of the elastomer under the action of a triaxial tension, whereas for weakly-bonded systems it appears to take place by detachment of the elastomer from the surface of the inclusion. Examples of these failure processes are shown in Fig. 2. The precise criteria for either process to occur are not really well understood, however. At what level of bonding is one process superseded by the other? Does the failure stress for either process depend upon the size of the inclusion? And how are these processes altered when inclusions are placed in close proximity? Experiments designed to address these questions have now been carried out, using transparent elastomers containing small glass beads. The diameter of the beads was varied over a wide range, 60 to 5000 μm. The strength of adhesion between a bead and the elastomeric matrix was also adjusted by treating the bead with either a coupling agent or a release agent before use. Several different elastomers were employed. In each case the elastic modulus was varied by varying the degree of molecular interlinking; values of Young's modulus E were obtained in this way ranging from 0.9 to 3.0 MPa. Observations of various failure processes and experimentally determined values of the corresponding failure stresses are reported below.

2. Experimental details

2.1. Elastomers

Several different elastomers were used in the experiments: two types of polybutadiene (Cis-4

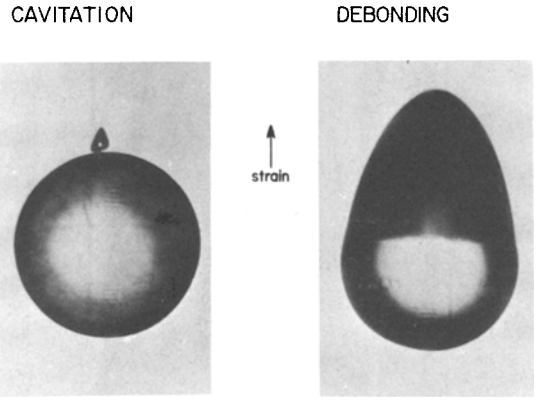

Figure 2 Cavitation and debonding at the surface of a spherical inclusion in an elastic matrix under tension. Direction of applied tension: vertical. Diameter of inclusion: 1.2 mm.

1203, Phillips Petroleum Company, and Diene 35 NFA, Firestone Rubber and Latex Company), two types of *cis*-polyisoprene (SMR-5L, Malaysian natural rubber, and Natsyn 2200, Goodyear Tire and Rubber Company) and a castable silicone rubber compound (Sylgard S-184, Dow Corning Corporation). The first four materials were cross-linked by adding various amounts of dicumyl peroxide and then heating the mixture in a mould to produce cross-linked rubber slabs containing one or two centrally-located glass beads, inserted before cross-linking. The silicone rubber was cross-linked using a reagent (Sylgard C-184) supplied by Dow Corning Corporation, which was added to the elastomer in various proportions. The mixture was then poured into a glass tray and cross-linked by heating for 24 h at 110° C. Glass beads were placed in the centre of the sheet after 15 min, i.e. before much cross-linking had taken place.

All of these materials had in common a high degree of transparency, so that cavitation near, or detachment from, the inclusion could be observed directly (Fig. 2).

2.2. Rigid spherical inclusions

Soda-lime glass beads were used as rigid inclusions. They were washed with boiling isopropyl alcohol, dried, and inserted in the centre of the rubber strips before cross-linking them. In order to obtain strong adhesion to diene elastomers, some beads were treated with a dilute solution of vinyltriethoxysilane in water, using acetic acid as a catalyst for hydrolysis of the ethoxy groups. They were then heated for 30 min at 110° C. To obtain poor adhesion to diene elastomers, ethyltriethoxysilane was used instead of the vinyl silane. The vinyl group appears to form a covalent bond with the elastomer during cross-linking with dicumyl peroxide, but the ethyl group does not [7].

In order to obtain strong and weak adhesion to the silicone elastomer, glass beads were treated with a special primer (92-023, Dow Corning Corporation) and a dilute solution of non-ionic surfactant (Triton X-405) in ethanol, respectively.

2.3. Measurement of failure stresses

Measurements were made of the applied tensile stress t_c at which the first visible cavity appeared, and of the stress t_a at which sudden debonding occurred, if debonding took place before any cavity formed. These stresses were applied to the ends of a long parallel-sided strip of the elastomer, having the inclusion at its centre. The thickness and width of the strip were at least three times the diameter of the inclusion, and usually much larger, so that the inclusion was effectively contained within an infinitely large block, subjected to simple extension. Quite large extensions, of the order to 50 to 400 per cent, were imposed before failure. They were especially large for cavitation near a small-diameter inclusion, well-bonded to a soft elastomeric material. Now, rubbery materials generally follow non-linear relationships between tensile stress and extension, as shown in Fig. 3 for some of the materials used in the present experiments. Values of Young's modulus E can be obtained from the initial slopes of such relationships, but the stresses near an inclusion calculated from linear elasticity theory are unlikely to be accurate for non-linear materials when the imposed strains are large. It should be noted that Oberth and Bruenner [4] used engineering stress (applied force per unit of unstrained cross-sectional area) in comparing their measured cavitation stresses with theoretical predictions. As their materials were stretched significantly under these stresses, by 50 to 100 per cent, the true applied stresses were considerably larger than the values they quote, by the same proportion.

In Fig. 4, the relationship between true tensile stress t and extension e are shown for some of the elastomers used. These relationships are

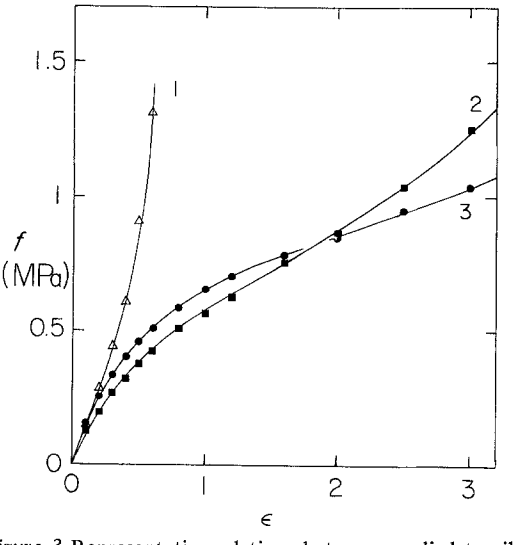

Figure 3 Representative relations between applied tensile force f per unit undeformed cross-sectional area and extension e. 1, S-184; 2, SMR-5L; 3, Cis-4.

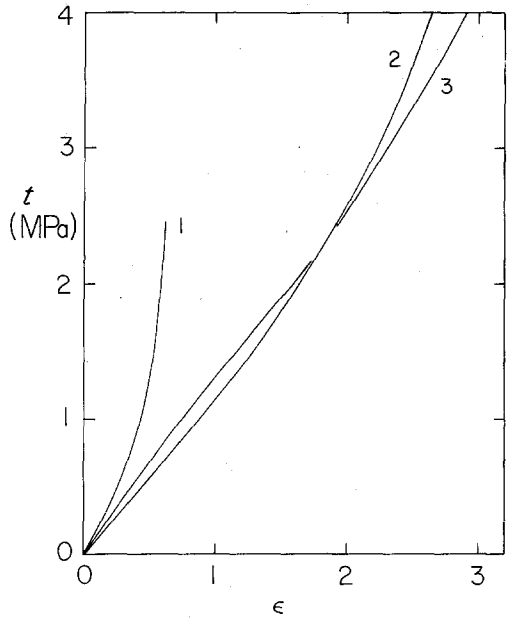

Figure 4 Representative relations between tensile stress t and extension e. 1, S-184; 2, SMR-5L; 3, Cis-4.

substantially linear in many cases, even up to strains of 200 to 300 per cent. Thus, the conclusions of linear elasticity theory might well apply, at least to a first approximation, to the high stresses set up near a rigid inclusion in a highly stretched elastomer.

3. Experimental results and discussion

3.1. Failure processes with a single inclusion

With well-bonded inclusions a small cavity formed near one pole of the inclusion in the direction of the applied tension (Fig. 2a), when the applied stress reached a critical level. On further elongation the cavity grew in size to touch the glass bead and several other cavities appeared at both poles (Fig. 5). They grew somewhat in the tension direction as the strain was increased further until the test piece broke in two, usually initiated from a cavity.

With less well-bonded inclusions an abrupt debonding took place after the cavities had already appeared, as shown in Fig. 6. In these cases, a lateral crack was sometimes observed to form subsequently in the elastomer near the edges of the debonded region. It grew slowly until it escaped from the immediate vicinity of the inclusion, when catastrophic failure ensued.

With unbonded inclusions the initial failure event was a sudden detachment at one side of the inclusion (Fig. 2b), followed at much larger strains by the appearance of a smaller debonded void at the other side of the inclusion (Fig. 7). Fracture again resulted from the growth of a lateral crack, initiated near the edge of the debonded region.

3.2. Cavitation stresses

The critical value of the applied force f_c per unit undeformed cross-sectional area at which the first cavity was observed, is plotted in Fig. 8 against Young's modulus E, for five different materials. At first sight, these results appear to be in reasonable agreement with the theoretical predictions of Oberth and Bruenner, represented by the broken line in Fig. 8. However, the use of nominal applied stress in place of true tensile stress does not seem appropriate. There are substantial quantitative differences between these two measures of stress for highly deformed materials, so that the apparent agreement shown in Fig. 8 is lost when true stresses are employed, as shown

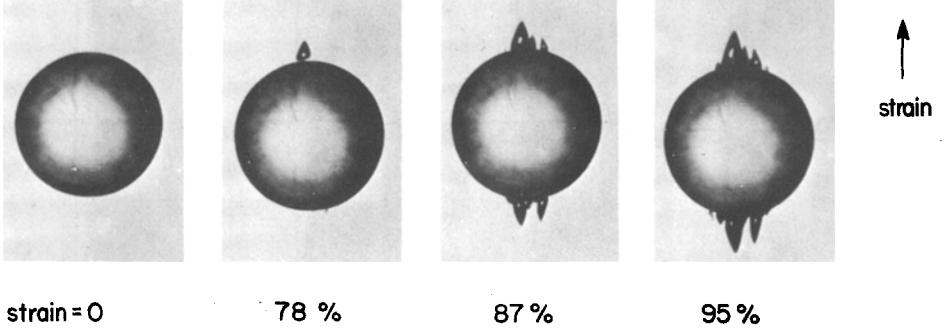

Figure 5 Progress with increasing tensile strain of cavitation in a silicone elastomer (S-184) $E = 0.9$ MPa, containing a glass bead of 1.22 mm diameter bonded to the elastomer with a primer.

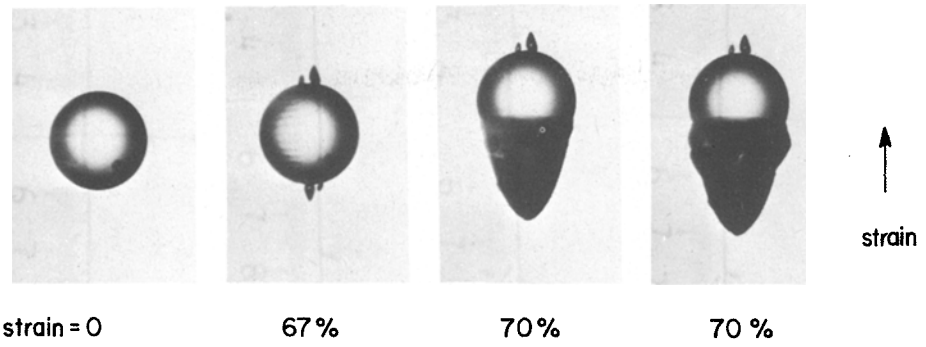

Figure 6 Progress with increasing tensile strain of cavitation in a silicone elastomer (S-184) $E = 2.2$ MPa, containing an untreated glass bead of 610 μm diameter.

in Fig. 9. Furthermore, the stresses at which cavitation occurs near small inclusions are much greater than for large ones, as discussed below, so that the apparent numerical agreement shown in Fig. 8 fails to hold for inclusions of other sizes.

When the true stresses t_c for cavitation are plotted against the corresponding values of Young's modulus E, linear relationships are obtained with slopes approximately equal to the theoretical value 5/12, but displaced to higher stresses as the diameter of the inclusion is reduced (see Fig. 9 and 10). Moreover, the stresses for cavitation in Natsyn 2200 appear to be significantly higher than for all the other materials under similar conditions. This feature is discussed later.

It was found that all of the cavitation stresses could be represented quite well by a relationship of the Hall–Petch form [8, 9]:

$$t_c = AE + Bd^{-1/2} \qquad (1)$$

where A and B are constants and d denotes the diameter of the glass bead. Some representative results are plotted in this way in Fig. 11; satisfactorily linear relations were obtained, with slopes B of 40 kPa·m$^{1/2}$ for Natsyn 2200 and 25 kPa·m$^{1/2}$ for all of the other elastomers, and an intercept corresponding to a value of A of about 0.5.

The term AE in Equation 1 is attributed to the elastic resistance to infinite expansion of a small spherical void in an elastomer subjected to triaxial tension [5]. It is hypothesized that such microscopically small voids exist in all elastomers. Moreover, it is known that the stress field near the poles of a rigid spherical inclusion is a triaxial tension, of magnitude $2t_\infty$ where t_∞ is the tensile stress applied at infinity (see Fig. 1). Thus, a failure criterion for cavitation of the form

$$t_c = 5E/12 \qquad (2)$$

is expected to be generally applicable [4]. However, it now appears that this criterion is only valid for relatively large inclusions. It becomes increasingly inadequate as the size of the inclusion is reduced and the second term on the right-hand-side of Equation 1 becomes increasingly important.

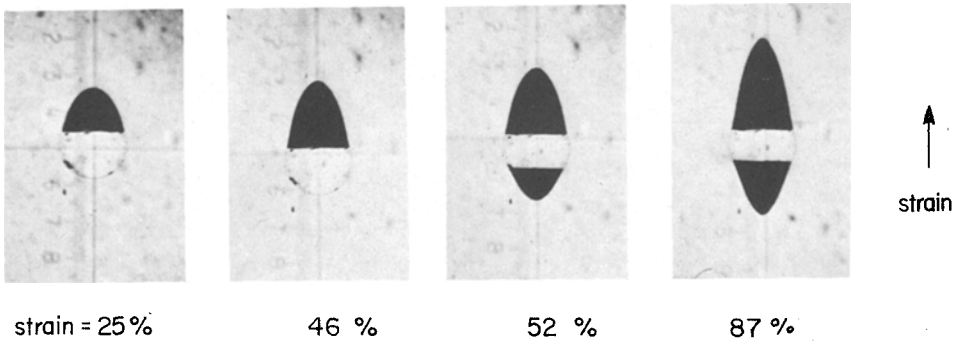

Figure 7 Progress with increasing tensile strain of debonding in natural rubber (SMR-5L) $E = 1.6$ MPa, containing an ethylsilane-treated glass bead of 610 μm diameter.

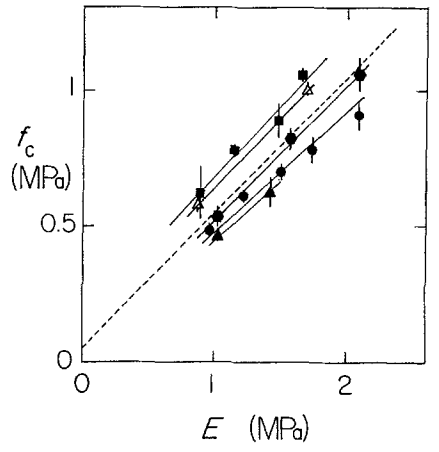

Figure 8 Nominal tensile stress f_c (force per unit of undeformed cross-section) at which the first cavity was observed in five elastomers containing a glass bead of diameter 600 μm, plotted against Young's modulus E. ■ Natsyn 2200; △ S-184; ● SMR-5L; • Cis-4; ▲ Diene 35 NFA.

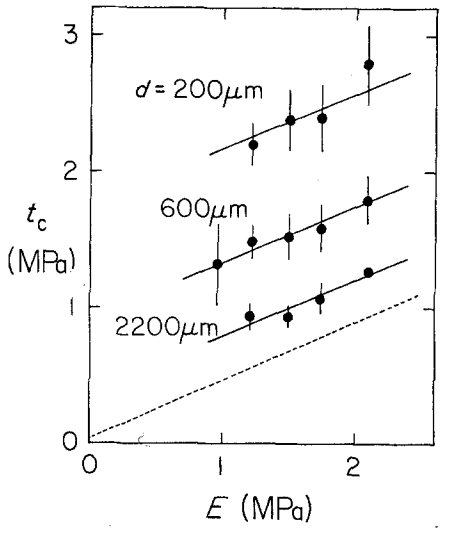

Figure 10 Applied tensile stress t_c for void formation against Young's modulus E for samples of Cis-4 containing glass beads of various diameters d. The dotted line represents the theoretical relation, Equation 2.

This second term resembles the Griffith criterion [10] for growth by tearing of a small circular crack of diameter c in the material close to the inclusion, where the tensile stress is $2t$ [6],

$$2t_c = (2\pi EG_c/3c)^{1/2} \quad (3)$$

In this relationship G_c denotes the energy required to propagate a crack by tearing through unit area of material. Values of the tearing energy G_c were measured for the various elastomers. They were found to range from about 500 to about 5000 J m^{-2}.

Thus, it appears that the formation of a visible cavity near a small inclusion of diameter d involves the growth by tearing of a small defect of diameter c, where c is found to be proportional to d. Putting $c = \alpha d$ to denote this proportionality, the magnitude of the constant α can be estimated by comparing the experimental values of the slopes B in Equation 1 with the predictions of Equation 3. When this is done, using a representative value for E of 1.5 MPa, the value obtained for α is found to be improbably large, of order unity. Defects comparable in size to the inclusion itself would certainly not escape notice in the experiments.

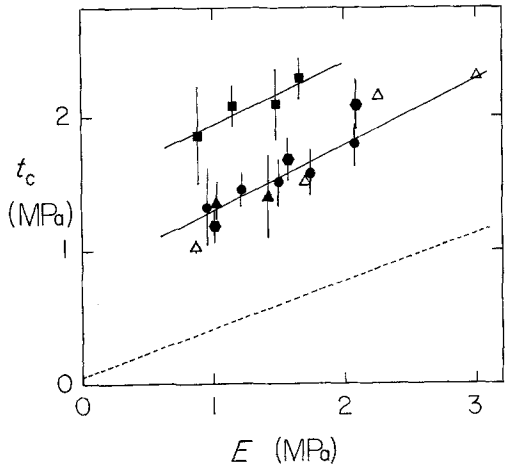

Figure 9 Applied tensile stress t_c at which the first cavity was observed in five elastomers containing a glass bead of diameter 600 μm, plotted against Young's modulus E. The symbols have the same significance as in Fig. 8.

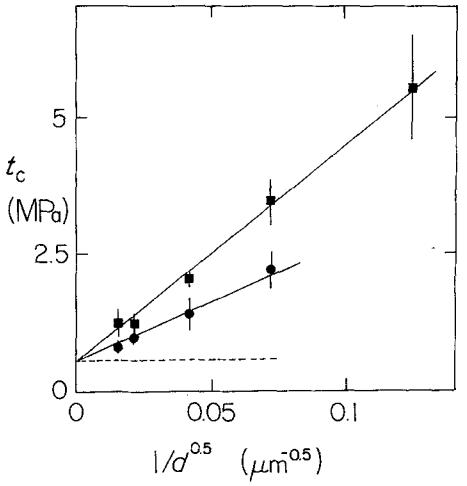

Figure 11 Applied tensile stress t_c for void formation against $d^{-1/2}$, where d is the diameter of the glass bead inclusion. ■ Natsyn 2200; • Cis-4.

It is therefore concluded that Equation 3 does not hold for the propagation of a small crack near a rigid inclusion in an elastomer under tension.

Several reasons for this failure can be postulated. The elastomer near the inclusion is not under a simple tensile stress, and Equation 3 may be invalid in this case. The initial defects are inherently small and values of G_c obtained by tearing apart large specimens may not apply to microscopic tearing processes. Also, it is known that stretched elastomers tear much more easily in the stretching direction so that much lower values of G_c will apply to tears running in the direction of the applied tension [11]. Whatever the reason, it is clear that there is a strong dependence of the critical stress for cavitation upon the size of the rigid inclusion and that the critical stresses, although quite large for small inclusions, are unexpectedly low when a Griffith tearing criterion is applied (Equation 3).

The cavitation stresses are significantly higher for Natsyn 2200 than for the other elastomers examined and this observation may provide a useful clue to the origin of the size dependence. Although Natsyn 2200 is closely similar to natural rubber (SMR-5L), it does not crystallize as readily on stretching. Consequently, it probably shows a different level of anisotropy of tear strength in the stretched state. A further experimental study of this feature would be illuminating.

3.3. Debonding stresses

Observations were also made of the critical applied stress t_a at which the elastomer pulled away from a weakly bonded inclusion. For an inclusion of a given size, the debonding stress was found to be smaller for harder elastomers, in marked contrast to the increase of cavitation stress t_c with elastomer modulus discussed in the preceding section. The two failure processes are thus quite distinct, as shown in Fig. 12.

It is at first sight surprising that the debonding stress should decrease with Young's modulus E of the elastomer, as shown in Fig. 12, because a simple Griffith treatment of the mechanics of debonding yields the relationship [12]

$$t_a = (8\pi E G_a / 3d \sin 2\theta)^{1/2} \qquad (4)$$

where G_a denotes the energy required to detach the elastomer per unit area of interface and 2θ denotes the angle subtended by a hypothetical initially debonded circular patch on the inclusion,

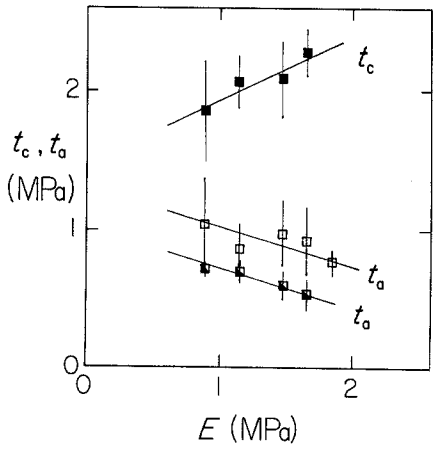

Figure 12 Applied tensile stress for void formation t_c or detachment t_a against Young's modulus E for samples of Natsyn 2200 containing a glass bead, diameter 600 μm. ■ Bonded; □ untreated; ▣ treated with ethylsilane.

located at the pole, i.e. in the direction of the applied tension. Equation 4 suggests that the debonding stress will increase with an increase in E. However, it is commonly found that the work G_a of detachment of an elastomer from a rigid surface is greatly dependent upon the dissipative properties of the elastomer, being greater for more dissipative materials [13]. Now, harder elastomers, obtained by incorporating a greater density of intermolecular bonds, are less dissipative than softer materials and show a lower strength of adhesion [13, 14]. This was found to be the case also for the present materials. Thus, the term G_a in Equation 4 is reduced drastically as the term E is increased and the net effect is a reduction in debonding stress as the elastomer is made harder.

Since the detachment energy G_a is also strongly dependent upon the rate of detachment, it is rather difficult to make a quantitative comparison with the predictions of Equation 4. If it is assumed that the rate of propagation of the initial debond is about 10^{-5} m sec^{-1}, then the measured value for G_a of about 17 J m^{-2} for a silicone elastomer S-184 peeled from a detergent-treated glass plate at this rate leads to a value for the subtended angle θ of about 7.5°, using the measured debonding stress for a 200 μm bead of about 2 MPa, and Young's modulus for this elastomer of about 2.2 MPa, in Equation 4.

This value of θ is a measure of the area of the hypothetical initially debonded patch upon the surface of the inclusion which grows in a catastrophic way when the applied tensile stress

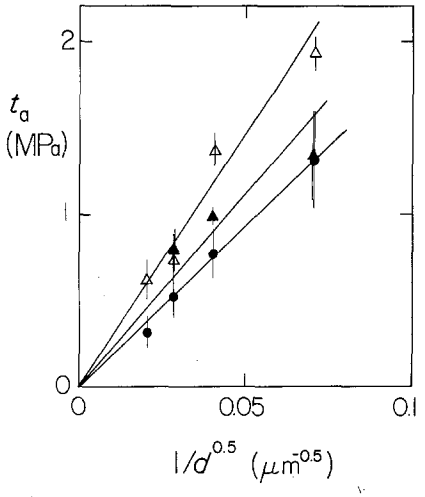

Figure 13 Applied tensile stress t_a for debonding against $d^{-1/2}$, where d is the diameter of the glass bead inclusion. △ S-184; ▲ Diene 35NFA; • Cis-4.

reaches the critical value t_a. When inclusions of different size were used, the debond stress t_a was found to vary markedly, being much larger for smaller inclusions, as discussed later. Surprisingly, these results are consistent with a substantially constant value for θ, independent of the size of the inclusion. This suggests that θ does not, in fact, represent a specific defect at the interface between the elastomer and the inclusion, because it seems highly unlikely that the area of a debonded patch would prove to be proportional to the surface area of the inclusion itself, over wide ranges of size. Instead, it seems likely that θ represents a characteristic feature of the mechanics of debonding from spherical inclusions. It is interesting to note that a similar (constant) value of θ, of about 18°, was deduced from studies of the glass continuum from spherical thoria inclusions under the action of stresses arising from differential thermal contraction [15].

Measured values of debonding stress t_a are plotted in Fig. 13 against the diameter of the glass bead raised to the negative half-power, in accordance with Equation 4. Results for three different elastomers are shown. In all cases, the debonding stress was found to increase as the size of the inclusion was decreased, approximately in accordance with a negative half-power. Thus, as for cavitation stresses, debonding stresses also appear to follow a Griffith-type relationship in terms of the size of the inclusion. However, the slopes of the relationships shown in Fig. 13 are somewhat smaller than those for cavitation (Fig. 11) and the relationships appear to pass through the origin, rather than extrapolating to yield a finite value of t_a for infinitely large inclusions.

3.4. Failure processes with two inclusions

The progress of cavitation in the vicinity of two inclusions having their centres arranged along the tension axis took a characteristic and distinctive form. First, at a critical stress somewhat lower than that necessary to cause a void to appear near an isolated inclusion, small cavities formed near the inner poles (Fig. 14). Apparently, the triaxial stress developed at these points is somewhat greater than $2t$ when the inclusions are closely spaced.

Then, at a somewhat higher value of applied stress, a large cavity suddenly appeared midway between the two inclusions. A similar phenomenon takes place in thin elastomer cylinders bonded between rigid plates and placed under tension [5]. It is attributed to the unbounded expansion of an initially present microscopic

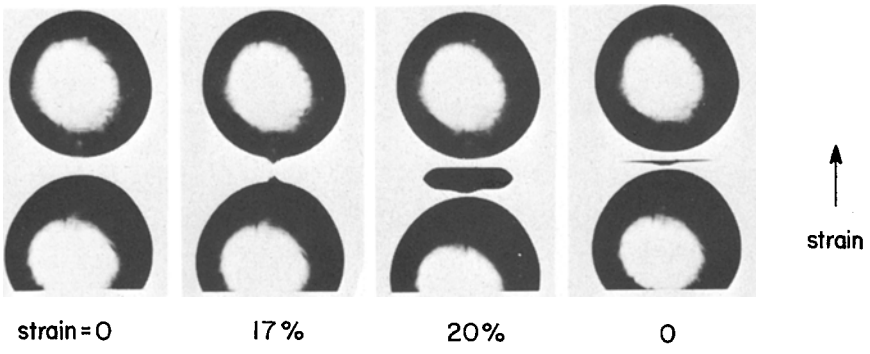

Figure 14 Progress of cavitation in a silicone elastomer, $E = 2.2$ MPa, containing two glass beads of 1.25 mm diameter bonded to the elastomer. Direction of applied tension: vertical.

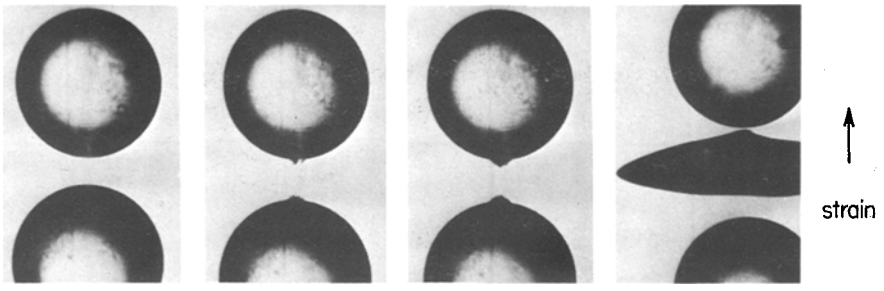

Figure 15 Progress of cavitation in a silicone elastomer, $E = 3.0$ MPa, containing two glass beads of 1.25 mm diameter bonded to the elastomer. Direction of applied tension: vertical.

void under the action of the triaxial tension present in the interior of the cylinder. Apparently, a similar stress field is developed between two rigid spherical inclusions and also leads to the formation of a large void.

The second cavity was found to be quite stable, growing slowly as the applied stress was increased (Fig. 14), until it emerged from the gap between the two inclusions. At this point it grew catastrophically, leading to rupture of the specimen.

A second example of cavity formation between two inclusions is shown in Fig. 15. In this case the spacing of the inclusions was rather larger and the final cavity grew rapidly, causing rupture.

From these observations it seems clear that tensile rupture of specimens containing rigid inclusions is generally caused by the second cavitation process, occurring between inclusions, rather than the first, occurring near the poles of isolated inclusions. The latter cavities only grow in the direction of the applied tension, as shown in Fig. 5, and thus do not lead directly to rupture.

4. Conclusions

The existence of two distinct failure phenomena, cavitation and debonding, has been clearly demonstrated using transparent elastomers containing glass beads of various sizes.

The critical stress for cavitation was found to depend on the Young's modulus of the elastomer and on the diameter of the glass bead. By extrapolation, the critical stress for cavitation near an infinitely large bead is found to be linearly dependent on the Young's modulus of the elastomer, $t_c = 5E/12$, in accordance with a simple theory of cavitation in which surface and fracture energies are neglected [5]. The dependence of the cavitation stress on the diameter of the bead takes a Griffith form, being proportional to the negative half-power of the bead diameter. However, the measured stresses are lower than expected for precursor defects much smaller than the inclusion itself, as observation requires. This anomaly calls for further study.

The critical stress for debonding increases as the strength of adhesion between the elastomer and the bead was increased, as predicted by theory. On the other hand, it decreased with increasing Young's modulus of the elastomer. This anomaly is attributed to a decrease in the strength of adhesion between the elastomer and the bead as the Young's modulus of the elastomer is increased. It was also found that the critical stress for debonding was strongly dependent on the diameter of the bead, in accord with a Griffith-type relation:

$$t_a = (8\pi E G_a / 3d \sin 2\theta)^{1/2}$$

This suggests that the effective initial debond angle θ is approximately independent of the diameter of the bead, $\theta = 10^\circ \pm 5^\circ$. This implies that θ does not represent a real defect at the surface of the inclusion, but a mechanical feature of debonding from a spherical surface.

For two beads in close proximity, a second cavitation process was observed midway between them, at a stress which decreased as the distance between the beads was decreased. This second cavity grew at right angles to the applied stress and led to catastrophic rupture of the specimen once it had escaped from the restraining influence of the inclusions. In contrast, cavities and debonds formed at the poles of isolated inclusions, grew in the direction of the applied tension, so that they did not lead directly to rupture.

Acknowledgements

This work was supported by a research grant from the Office of Naval Research (Contract N00014-76-C-0408), and a research fellowship from Cabot Corporation.

References

1. H. F. SCHIPPEL, *Industr. Eng. Chem.* **12** (1920) 33.
2. H. A. DEPEW and M. K. EASLEY, *ibid.* **26** (1934) 1187.
3. C. MARKINS and H. L. WILLIAMS, *J. Appl. Polym. Sci.* **18** (1974) 21.
4. A. E. OBERTH and R. S. BRUENNER, *Trans. Soc. Rheol.* **9** (1965) 165.
5. A. N. GENT and P. B. LINDLEY, *Proc. Roy. Soc. (London)* **A249** (1959) 195.
6. J. N. GOODIER, *Trans. ASME* **55** (1933) 7.
7. A. AHAGON and A. N. GENT, *J. Polym. Sci. Polym. Phys. Ed.* **13** (1975) 1285.
8. E. O. HALL, *Proc. Phys. Soc. (London)* **64B** (1951) 747.
9. N. J. PETCH, *J. Iron Steel Inst. London* **174** (1953) 25.
10. R. A. SACK, *Proc. Phys. Soc. (London)* **58** (1946) 729.
11. A. N. GENT and H. J. KIM, *Rubber Chem. Technol.* **51** (1978) 35.
12. A. N. GENT, *J. Mater. Sci.* **15** (1980) 2884.
13. A. N. GENT and R. P. PETRICH, *Proc. Roy. Soc. (London)* **A310** (1969) 433.
14. A. N. GENT and G. R. HAMED, *Plast. Rubber: Mater. Appl.* **3** (1978) 17; reprinted in *Rubber Chem. Technol.* **51** (1978) 354.
15. Y. M. ITO, M. ROSENBLATT, L. Y. CHENG, F. F. LANGE and A. G. EVANS, *Int. J. Fract.* **17** (1981) 483.

Received 31 August
and accepted 21 September 1983